ELSEVIER

Biochimica et Biophysica Acta 1273 (1996) 150–158

BBA Biochimica et Biophysica Acta

Changes in light energy distribution upon state transitions: an in vivo photoacoustic study of the wild type and photosynthesis mutants from *Chlamydomonas reinhardtii*

René Delosme [a,*], Jacqueline Olive [b], Francis-André Wollman [a]

[a] *Institut de Biologie Physicochimique, 13 rue Pierre et Marie Curie, 75005 Paris, France*
[b] *Institut Jacques Monod, Université Paris VII, 2 place Jussieu, 75251 Paris Cedex 05, France*

Received 5 July 1995; revised 3 October 1995; accepted 18 October 1995

Abstract

We investigated, by a photoacoustic method, the changes in light energy distribution to the reaction centres upon state transitions in vivo in *Chlamydomonas reinhardtii*. We present spectra of the quantum yield of charge separation in the wild type and in several photosynthesis mutants lacking either cytochrome b_6f complexes, the PS II cores or the PS I cores. Our results show unambiguously that in the wild-type LHCII becomes connected to PS I in state 2, in a cyt b_6f-controlled process. We show that mutants lacking the PS II cores, but not those lacking PS I cores, display a behaviour very similar to that of the wild type upon state transition. Lateral displacement of LHCII, but not of minor antenna complexes (CP26), from the stacked to the unstacked membrane domains results in transfer to PS I of about 80% of the excitation energy absorbed by LHCII. Consequently, in state 2, more than 90% of the chlorophylls transfer energy to PS I in mutants lacking PS II cores. In contrast, a significant proportion of the PS I peripheral antenna is connected with PS II, in state 1 as well as in state 2, in mutants lacking PS I cores. Moreover, in these mutants, phospho-LHCII remains part of PS II antenna in state 2. We attribute these features to the super-stacked organization of the thylakoid membranes in the PS I deficient mutants.

Keywords: Excitation transfer; State transition; Quantum yield spectrum; Light-harvesting complex; Photoacoustics

1. Introduction

In their pioneering work from the late 60's, Murata [1] and Bonaventura and Myers [2] established, as a core concept of state transitions, that a photosynthetic cell is able to change the distribution of absorbed light energy between the two photosystems. A number of issues raised by these studies, have since been addressed successfully (reviewed in [3,4]). The most spectacular one has been the determination of the molecular basis for the changes in light energy distribution: the supramolecular organization of LHCII, the major peripheral antenna complex, is controlled by the reversible phosphorylation of some LHCII subunits, which causes migration of the antenna proteins between the stacked membrane domains, enriched in PS II, and the stroma lamellae domains, enriched in PS I. Although the dissociation of part of the phospho-LHCII complexes from PS II is nowadays widely accepted, the actual association of phosphorylated antenna with PS I remains a matter of controversy (discussed in [4] and references therein, see also [5,6].

Most of these studies, whether biochemical or functional, were performed with higher plant chloroplasts, which display state transitions of limited amplitude. This is at variance with state transitions in the green alga *C. reinhardtii*, which produce room-temperature fluorescence changes about 2–3-times larger than in higher plants [7,8]. We used this material to compare in vivo, by a photoacoustic method recently developed [9], the quantum yield of PS I and PS II charge separations in state 1 and in state 2. This approach allows one to detect over a wide range of wavelengths any changes in the efficiency of transfer of an absorbed quantum to the reaction centres. In the present study, we compare the excitation transfer efficiencies in conditions known to promote state 1 or state 2, in the wild

Abbreviations: WT, wild type; LHC, light-harvesting complex; CC, core complex; PS, Photosystem; Chl, chlorophyll; cyt, cytochrome; PQ, plastoquinone.; RT, room temperature; TAP, Tris-acetate-phosphate; BQ, benzoquinone; DMSO, dimethylsulfoxide; DCMU, 3-(3,4-dichlorophenyl)-1,1-dimethylurea.

* Corresponding author. Fax: +33 1 40468331.

SSDI 0005-2728(95)00143-3

type of *C. reinhardtii* and in mutant strains lacking cyt b_6f complexes or PS II or PS I cores.

2. Materials and methods

2.1. Strains

The WT and mutant strains from *C. reinhardtii* were grown to mid-exponential phase in TAP medium under 300 lux illumination. Mutants FUD7 and F34 [10] lack the PS II cores; mutants M18 [11] and C3 [12] lack the PS I cores; mutants FUD6 [13] and ac206 [14] lack the cyt b_6f complexes. Double mutants were named after the single mutants used in crosses.

2.2. State transitions

Unless otherwise indicated, state transitions were performed in the dark. State 1 conditions (PQ pool oxidized) corresponded to strongly aerated cultures, and state 2 conditions (PQ pool reduced) were achieved by placing the algae in anaerobic conditions, either in situ by a mere incubation in the photoacoustic cuvette, or by a 20 min exposure to glucose/glucose oxidase as described in [7]. p-BQ fixation of the algae in either of the two states was used when required [15]. In vivo incorporation of ^{32}P in the thylakoid membrane polypeptides was performed according to previously published procedures [7,8].

2.3. Photoacoustic spectroscopy

All the photoacoustic measurements were performed at 22°C. The cells of *C. reinhardtii* were concentrated by a factor of 500 to 1500 before photoacoustic measurement. The spectral dependence of the photochemical activity (charge separation) induced by a 3 ns laser flash was measured in the first microsecond following the flash, using the photoacoustic method described in [9]. The laser dyes used were 7 mM DCM in the 630–690 nm range, and 10 mM LDS 698 beyond 695 nm (solvent: DMSO). According to [9], the quantum yield of the overall energy-conversion process (i.e., the number of charge separations per absorbed photon) was measured in relative units by the quantity

$$Y = \frac{I_L - I_D}{I_L} \times \frac{1240}{\lambda_{nm}},$$

where I_L is the acoustic signal measured while the reaction centres are closed by saturating continuous illumination in the presence of DCMU and hydroxylamine, I_D is the acoustic signal measured in fully active, dark-adapted material, and $1240/\lambda_{nm}$ is the energy of one light quantum expressed in eV. The overall efficiency measured by Y includes two factors: the probability for an absorbed light quantum to be trapped by a reaction centre, multiplied by the probability for the trapped exciton to give rise to a charge separation. The first term is related to the optical cross section, whereas the second one relates, strictly speaking, to the quantum yield of the photoreaction. We emphasize that Y must in no way be regarded as an absolute measurement of the energy storage efficiency, because the acoustic signal I_D measures the sum of two types of flash-induced pressure changes [9]. One of them arises from the thermal expansion of the medium (ΔV_{th}) and measures the amount of light energy which is degraded to heat. The second one results from a contraction (ΔV_{conf}) probably related to electrostriction. Contrary to ΔV_{th}, which is subject to internal calibration using a photochemically inactive sample as a thermal reference, ΔV_{conf} cannot be easily calibrated. However, we demonstrated [9] that both components ΔV_{th} and ΔV_{conf} are linearly related to the number of flash-induced charge separations. Accordingly, Y is proportional to the overall quantum yield of the light-energy conversion process, and can be used as a suitable measure of the photochemical efficiency.

In the present study, we investigated the spectral dependence of Y under different physiological conditions. In these experiments, each point of the quantum yield spectra resulted from integration of 20 to 10000 individual flash measurements, depending on the wavelength. The measuring flashes were spaced by 1 s in the spectral range where light is strongly absorbed by chlorophylls (630–690 nm), and 0.1 s in the far-red region, where absorption is very low (695–720 nm). As shown in Fig. 1a, we first checked that under our experimental conditions, the photochemical efficiency measured by Y (a) was not limited by the turnover rate of the reaction centres, and (b) was independent of the flash energy. The maximal incident light energy at the measuring cell was about 0.3 μJ cm^{-2} or 10^{12} photons cm^{-2}. The proportion of reaction centres hit during one flash was estimated as follows (Fig. 1b): Y was measured as a function of the number of successive flashes in a biological system (BBY particles treated with DCMU plus hydroxylamine) in which at least 90% of the centres can react only once. This system behaves as a 'photon counter' [16]. According to Fig. 1b, the maximal flash energy used in the present work corresponds to 1 photon per about 400 reaction centres, illustrating the high sensitivity of our photoacoustic technique.

2.4. Immunocytochemistry

The cells were fixed either in state 1 or state 2 conditions by *p*-benzoquinone treatment as described in [15], resuspended in TAP medium supplemented with 0.1 M sucrose and 10 mM $MgCl_2$, then broken through a Yeda press operating under 100 bar. The resulting broken cells were then pelleted and fixed in 3% paraformaldehyde and 1% glutaraldehyde in 4 mM potassium phosphate buffer

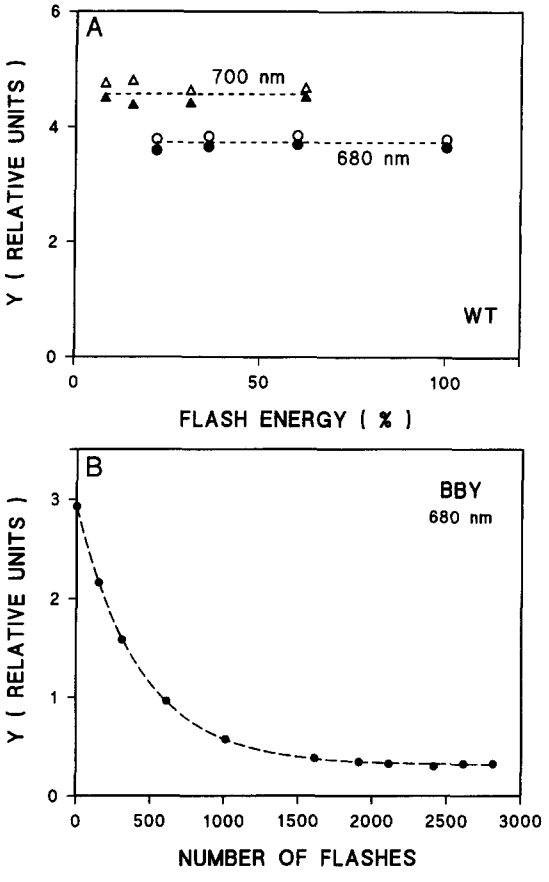

Fig. 1. (a) Flash-energy dependence of the overall quantum yield in untreated cells of *C. reinhardtii* (wild type). 100% is the maximal flash energy used at 680 nm in the present work (about 0.3 μJ cm^{-2}, or 10^{12} photons cm^{-2}). Note that Y is not limited by the time between flashes (solid symbols, 1 s; open symbols, 0.1 s). (b) Photochemical activity as a function of the number of flashes, in BBY particles treated with 40 μM DCMU plus 10 mM hydroxylamine. The initial value was measured in an untreated sample. Dashed line: exponential decay calculated from the experimental data. Flash energy: 100% (cf. (a)).

(pH 7.0). They were then dehydrated in ethanol and embedded in Lowicryl K4M. Thin sections were labelled with specific antisera (1/300 dilution) and with protein A-gold conjugates. Gold granules were counted over well-defined unstacked and stacked membranes, the length of which was measured on a Tektronix graphic tablet, yielding the

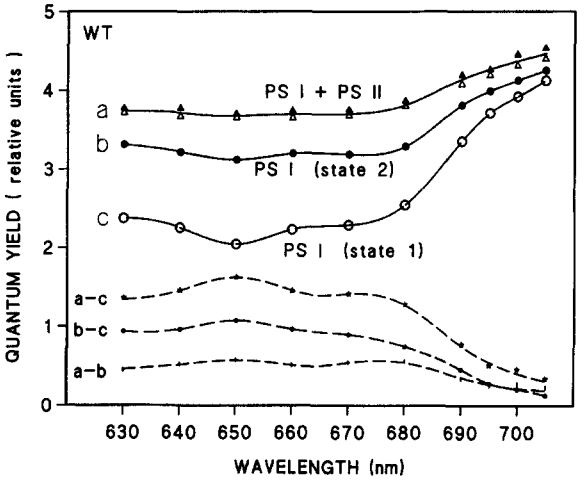

Fig. 2. Spectral dependence of the quantum yield in *C. reinhardtii* (wild type). Solid symbols, cells in state 2; open symbols, cells fixed in state 1. (a) Dark-adapted sample, no addition; (b) and (c) the cells were treated with 40 μM DCMU plus 10 mM hydroxylamine, and saturated with continuous light for 10 s. Then they were left for 3 min in the dark before the set of measurements.

labelling densities d_u and d_s of the two types of membrane.

3. Results

3.1. State transitions in the wild-type strain

In Table 1 are gathered fluorescence parameters which provide some typical features of state transitions occurring in vivo in the WT strain or various photosynthesis mutants from *C. reinhardtii*. As previously reported [7], transition from state 1 to state 2 in the WT, was accompanied by an extensive fluorescence quenching at room temperature, and a significant decrease in the 77 K fluorescence emission peak of PS II (685 nm) relative to that of PS I (717 nm). Using the photoacoustic technique, we measured the wavelength dependence of the quantum yield (in relative units) in dark-adapted cells of the wild type placed either in state 1 or in state 2 (Fig. 2). In curve a, the reaction centres of

Table 1
Typical fluorescence characteristics

		WT	$-b_6f$	−PS II	−PS II/b_6f	−PS I	−PS I/b_6f
F_{max} at RT [a]	State 1	100	100	100	100	100	100
	State 2	55	106	45	102	105	108
F_{PSII}/F_{PSI} at 77 K [b]	State 1	1.6	1.8	1.3	n.d.	0.37 [c]	n.d.
	State 2	1.1	1.7	0.7	n.d.	0.29	n.d.

[a] Maximal fluorescence yields at RT in state 2 are given relative to that in state 1 for each strain.
[b] F_{PSII} is taken as F_{686nm} emission in PS II core-containing strains and F_{682nm} (LHCII) in PS II core-lacking strains. F_{PSI} is taken as F_{717nm} emission in PS I core-containing strains and F_{707nm} emission (LHCI) in PS I core-lacking strains.
[c] Mean of three experiments.

both photosystems were active. As reported earlier [9], the overall quantum yield spectra are almost identical in state 2 and state 1. In this case, the photoacoustic technique does not distinguish the origin (PS I or PS II centres) of the charge separation. The similarity of the two spectra indicates that, in both states, the same number of absorbed light quanta are converted to chemical energy, regardless of the light energy distribution among the two types of reaction centre.

The charge separations occurring specifically in PS I centres were identified by inhibiting photoreaction II according to Bennoun [16]: in spectra b and c of Fig. 2, the cells were preilluminated a few seconds with continuous light in the presence of DCMU plus hydroxylamine before the set of measurements. Thus the PS II centres were blocked in the inactive Q_A^- state, and could not undergo any charge separation. All the remaining activity proceeded from the PS I centres. The quantum yield spectrum of the PS I centres in state 1 (curve c of Fig. 2) shows a strong depression centered around 650 nm, corresponding to the absorption maximum of Chl *b*. In this case, the efficiency of the PS I centres is about 55% of the overall efficiency (measured in curve a) in the same region, reflecting an almost equal distribution of excitation energy among the two types of reaction centres. This situation is similar to that observed in broken spinach chloroplasts [9], which are blocked in state 1 due to the oxidizing conditions which prevent LHC-kinase activity. In this case, LHCII transfers excitation essentially to PS II centres. In contrast, when cells were placed in state 2 (curve b of Fig. 2), the efficiency of the PS I centres in the 650 nm region was about 85% of the overall efficiency measured in curve a. This indicates that a large fraction of the PS II antenna transfers its excitation energy to PS I centres in state 2. When measured by the quantum yield at 650 nm, the cross-section increase of PS I upon transition from state 1 to state 2 was about 50%.

It has been shown previously that transition to state 2 in *C. reinhardtii* is accompanied by an increased phosphorylation of three LHCII subunits and two minor antenna complexes, CP26 and CP29 [17]. The latter are not phosphorylated upon transition to state 2 in higher plants. We therefore examined the possibility that the large state 1 to state 2 transitions in *C. reinhardtii*, would correspond to the migration of both LHCII and minor antenna complexes out of the PS-II-rich stacked membrane domains, to the PS-I-rich unstacked membrane domains. We therefore performed an immunocytochemical study of the distribution of both CP26 and LHCII upon state transition in the wild type. Table 2 shows the distribution of labelling densities of protein A-gold conjugates associated with antibodies against LHCII or CP26 between stacked (d_s) and unstacked (d_u) membrane regions in the two states. Since the average labelling densities (d_{ave}) varied from one experiment to another (see Discussion section), we focused on the changes in the ratio d_u/d_s of labelling densities between the two domains upon state transitions. In the wild-type strain, d_u/d_s [LHCII] increased about 3-times upon state 1 to state 2 transition, which is typical of a lateral displacement of LHCII upon phosphorylation [18]. In contrast, the minor antenna complex remained next to PS II, since d_u/d_s [CP26] was low in the two states and showed no increase upon transition to state 2.

This observation is reflected in the difference spectra corresponding to the various parts of the PS II antenna, taken from Fig. 2. The difference a − c reflects the quantum efficiency of the whole PS II antenna (LHCII, 'minor' antennae CP24, CP26 and CP29, and core complex CCII). The difference a − b corresponds to the 'fixed' PS II antenna, with a slight maximum near 680 nm due to CCII and probably the minor antennae, and another one at 650 nm which indicates that some LHCII (about 20%) remains attached to PS II. The difference b − c reflects the 'mobile' antenna, which in state 2 connects to PS I centres. Comparison of the 'fixed' and 'mobile' PS II antenna shows an enrichment in Chl *b* in the latter. This is consistent with the attribution of the mobile antenna to the sole LHCII, whereas the fixed PS II antenna also com-

Table 2
Lateral distribution of antenna proteins

	%stacking		State 1				State 2			
			d_{ave} [a]	d_s [b]	d_u [c]	d_u/d_s	d_{ave}	d_s	d_u	d_u/d_s
WT [d]	67	α-LHCII	1.9	2.5	0.7	**0.28**	2.9	2.9	2.8	**0.96**
		α-CP26	2.6	3.5	0.8	**0.23**	4.75	6.5	1.2	**0.18**
FUD7	65	α-LHCII	6.6	9.2	1.7	**0.18**	5.3	6.3	3.4	**0.54**
		α-CP26	3.1	3.8	1.7	**0.46**	2.2	3	0.8	**0.27**
C3	89	α-LHCII	1.4	1.5	0.7	**0.47**	1.3	1.3	1.2	**0.9**
ac206-M18	79	α-LHCII	0.7	0.7	0.6	**0.86**	0.85	1	0.8	**0.8**

[a] d_{ave}, the average labelling densities, are computed from the % stacking and the respective ([b]) d_s, labelling densities in stacked membrane domains, and ([c]) d_u, labelling densities in unstacked membrane domains. Since d_{ave} varies from one experiment to another, only changes in d_u/d_s should be used for comparison.

[d] WT, wild type; FUD7, PS II mutant; C3, PS I mutant; ac206-M18, cyt b_6f/PS I double mutant.

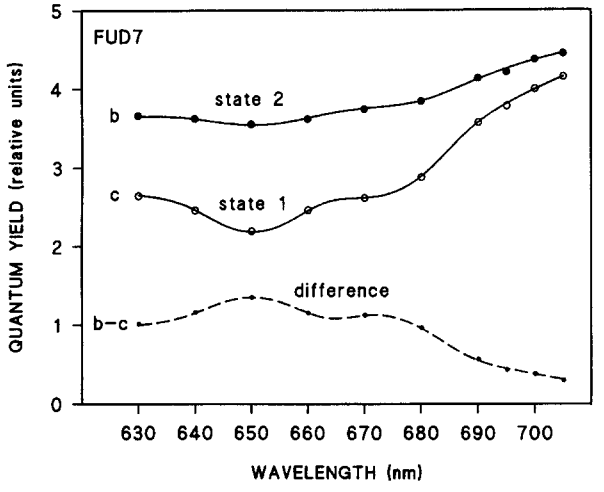

Fig. 3. Spectral dependence of the quantum yield in the CCII-deficient strain FUD7. b, cells in state 2; c, cells fixed in state 1.

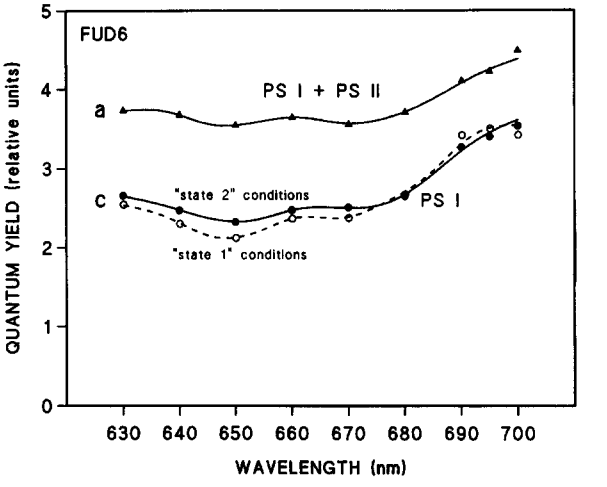

Fig. 4. Spectral dependence of the quantum yield in the cyt b_6f-deficient strain FUD6. Symbols as in Fig. 2.

prises the Chl *a* core antenna as well as the minor peripheral antennae, whose Chl *b*/Chl *a* ratio is lower than in LHCII [17].

3.2. State transitions in photosynthesis mutants lacking PS II cores

As documented previously [7,8], an extensive antenna reorganization still takes place upon state 1 to state 2 transitions in PS II mutants (see Table 1). Photoacoustic measurements further characterized the corresponding changes in exciton transfer efficiencies between the peripheral antenna and the PS I reaction centres. The marked state transitions occurring in these mutants are evidenced by the quantum yield spectra of Fig. 3 (b in state 2, and c in state 1). In state 2, the quantum yield spectrum of the FUD7 mutant was almost the same as the overall spectrum of the wild type (a in Fig. 2) – except for a scarcely more pronounced depression at 650 nm – proving that almost all the antenna pigments (including LHCII) were connected to PS I centres. When measured by the quantum yield at 650 nm, the cross-section increase of PS I upon transition from state 1 to state 2 was about 60%. As shown in Table 2, the changes in light energy distribution upon state 1 to state 2 transitions were accompanied by a 3-fold increase in d_u/d_s [LHCII] in the immunocytochemical study of FUD7. No such increase was observed for CP26 lateral distribution, which showed rather a decrease in d_u/d_s upon transition to state 2.

3.3. State transitions in photosynthesis mutants lacking cyt b_6f complexes

The same experiments were performed with mutant strains lacking the cyt b_6f complex, under conditions which normally favour either state 1 or state 2. As previously reported [19,20], Table 1 shows that in the two situations they display similar RT fluorescence yields and similar ratios of 77 K fluorescence emissions from PS II and PS I, with state 1 characteristics. The photoacoustic study of the single mutant FUD6 shows that the overall quantum yield spectrum (Fig. 4, curve a) resembles that of the wild type shown in Fig. 2 (curve a). But in contrast to the wild type, when the PS II centres were inhibited, the remaining quantum yield spectrum corresponding to the PS I centres was invariably typical of state 1, even under conditions which should normally lead to a complete transition to state 2. A similar spectrum (Fig. 5) was obtained in a double mutant strain (ac206.F34) lacking both PS II centres and cyt b_6f complex, indicating that these cells are also blocked in state 1. These data confirm that state transitions require the presence of the cyt b_6f complex [19,20]. Note that the PS I quantum yield spectra of Figs. 4 and 5, when compared with their equivalents in the cyt b_6f-containing strains (Figs. 2 and 3), present a

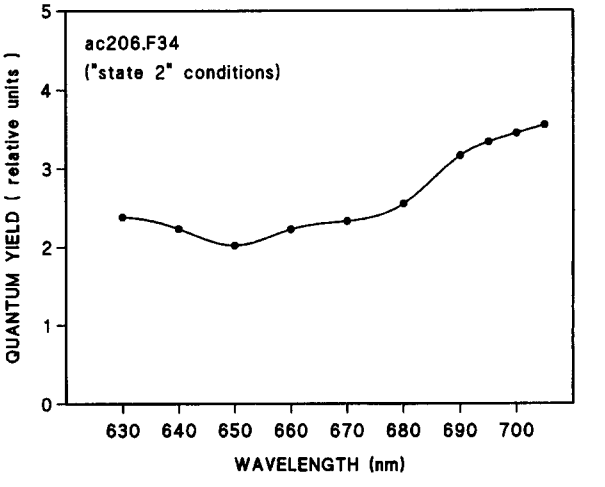

Fig. 5. Spectral dependence of the quantum yield under 'state 2' conditions in the double mutant strain ac206.F34, which lacks both CCII and cyt b_6f.

slightly deficient quantum yield in the far-red region. This deficiency was observed in all the cyt b_6f mutant strains that we have used.

3.4. State transitions in photosynthesis mutants lacking PS I cores

Table 1 shows that no quenching of the RT fluorescence yield occurs upon transfer of either a PS I single mutant or a PS I/cyt b_6f double mutant, from state 1 to state 2 conditions. Instead, as observed with cyt b_6f single mutants, state 2 conditions produce a slight increase at F_{max}. It reflects the reduced state of the plastoquinone pool, which acts as a weak fluorescence quencher in its oxidized form.

The phosphorylation pattern of thylakoid membrane proteins from these strains is shown for the two states in Fig. 6. The patterns of phosphoproteins are similar to those previously reported for thylakoid membrane proteins from *C. reinhardtii* [7,8]. Three PS II subunits, two minor antenna apoproteins and several LHCII subunits are distinctly labelled. In state 2, there is a general increase in polypeptide phosphorylation in the PS I single mutant, but not in the double mutant also lacking cyt b_6f complexes. Note that two LHCII subunits and a third polypeptide (diamonds in Fig. 6) are not labelled in the PS I mutant also lacking cyt b_6f. This is consistent with the phosphorylation pattern remaining in other single or double mutants lacking cyt b_6f complexes [20]. We conclude from the changes in phosphorylation patterns in the two strains upon state transitions that, in contrast to cyt b_6f complexes, PS I cores are not required for kinase activation. Accordingly, some decrease in PS II 77 K emission relative to that of the LHCI antenna at 707 nm [21] is observed in state 2 in the PS I single mutant (Table 1). The immunocytochemical detection of LHCII in the PS I mutant shows some increase in d_u/d_s [LHCII] in state 2 conditions (Table 2), whereas this ratio remains similar under state 1 and state 2 conditions in the PS I/cyt b_6f double mutant. However, the fraction of mobile LHCII in the PS I mutant should be low, owing to the superstacked organization of the thylakoids – about 90% stacking – in PS I mutants ([22,23] and Table 2).

Fig. 7 shows the quantum yield spectrum measured by photoacoustic spectroscopy in the mutant strain C3 lacking the PS I core, under conditions favouring either state 1 or state 2. No significant state transitions could be detected by this technique. The spectrum is practically the same in both situations, and indicates that the whole PS II antenna remains efficiently connected to the PS II reaction centres, under both state 1 and state 2 conditions. However, this spectrum differs significantly from that attributed to PS II in state 1 of the wild type (redrawn from Fig. 2, difference a – c). The higher value of the quantum yield, the lack of a definite peak at 650 nm (absorption maximum of chlorophyll *b*), and the relatively small 'red drop' in the far red region (only 1/3 of the maximal yield) prove that the absence of PS I core in the C3 strain is accompanied by significant energy transfer from LHCI to PS II reaction centres.

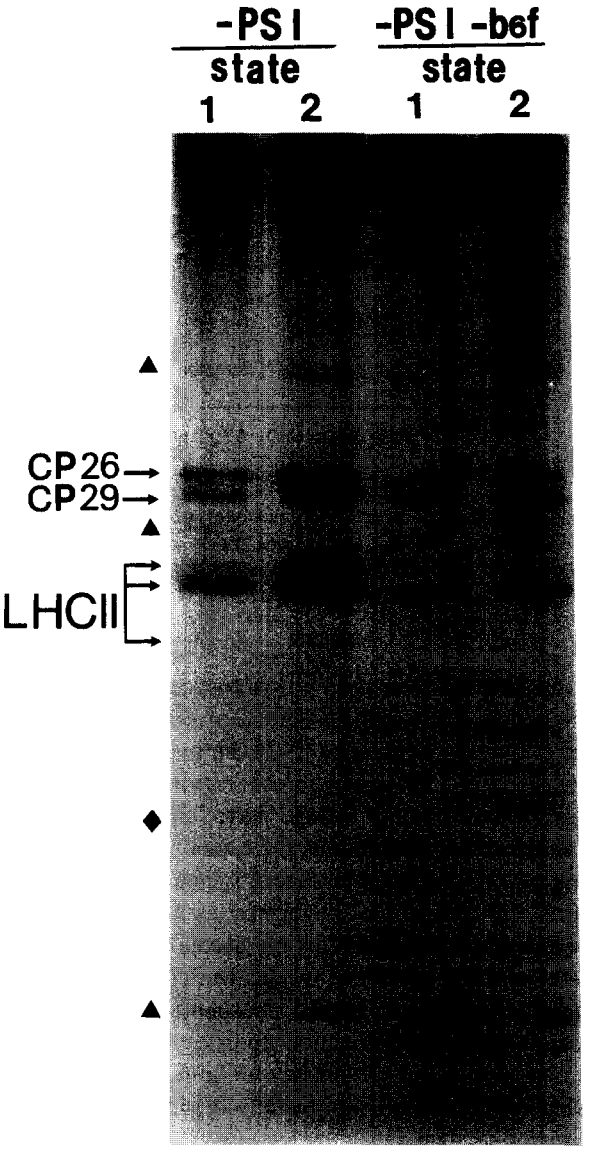

Fig. 6. Phosphopolypeptide patterns of the thylakoid membranes from the C3 mutant lacking PS I cores (−PSI), and the ac206M18 mutant lacking both the PSI core and the cyt b_6f complex (−PSI−b_6f). Cells were incubated with ^{32}P prior to incubation in state 1 or state 2 conditions. ▲,PS II subunits CP43, D2 and psbH product; ◆, phosphopolypeptide detected only in cyt-b_6f-containing strains.

4. Discussion

4.1. Photoacoustic studies provide unequivocal demonstration for complementary changes in LHCII association with PS I and PS II upon state transitions

State transitions are generally thought to maximize the quantum yield of energy conversion, by equilibrating light

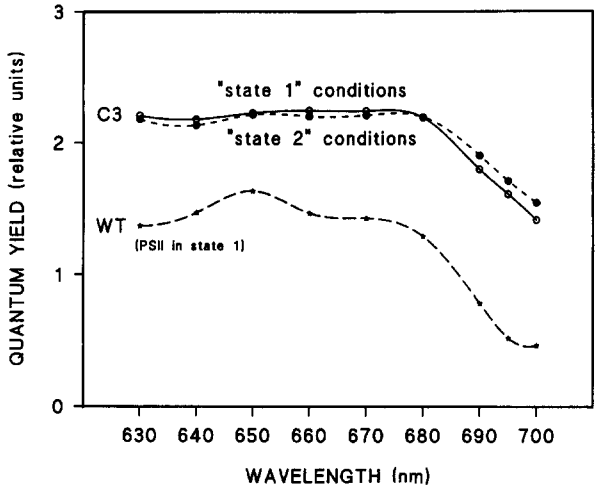

Fig. 7. Spectral dependence of the quantum yield in the CCI-deficient strain C3. Solid symbols, state 2 conditions; open symbols, state 1 conditions. The quantum yield spectrum of PS II in the wild type (state 1) was redrawn from Fig. 2 (difference a – c).

energy flux between the two photosystems. In this view, transition from state 1 to state 2 results in a decreased absorption cross-section of PS II centres with a concurrent increase in the absorption cross-section of PS I centres. Nevertheless, several authors have challenged this last point [4,24], considering that the excitation energy diverted from the PS II centres in state 2 is not redirected to PS I centres. Most often they suggested, as an alternative rationale for state transitions, that the decrease in PS II antenna size is part of a protective mechanism against excess PS II irradiation [4]. Disconnected phospho-LHCII would then undergo thermal deactivation upon excitation. Therefore, the overall quantum yield spectrum in the region of LHCII absorption should be significantly depressed in state 2 as compared to state 1.

Contrary to this prediction, we demonstrated in the present study that the overall quantum yield spectrum of the wild type (Fig. 2 curve a) is almost identical in state 1 and state 2. A similar conclusion was reached in other photoacoustic studies [25,26], except for a small loss of excitation energy (11–14%) reported by Canaani and Malkin [27] at 650 nm in state 2 of intact leaves (cf. Table 3).

On the other hand, our photoacoustic measurements detected a 50 to 60% increase in the quantum yield of PS I at 650 nm upon transition from state 1 to state 2. The quantum yield spectrum of PS I stimulation (difference b – c in Fig. 2 or 3) clearly reflects the contribution of LHCII, with a maximum at 650 nm due to Chl *b*, and a red-drop above 680 nm. These results are in agreement with the previous report by Delepelaire and Wollman [8] of a 50% change in PS I optical cross-section upon state transitions in another PS II mutant from *C. reinhardtii*. The suggestion by Allen and Melis [24], that this observation may be interpreted as mere consequence of the change in redox state of electron carriers in cyclic electron flow, is ruled out by the present study, which was performed under anaerobic conditions in both states, state 1 being preserved by p-BQ fixation.

Table 3
Light energy distribution between the two photosystems

Authors	State 1		State 2	
	PS II	PS I	PS II	PS I
[25]	0.75	0.25	0.56	0.44
[26]	0.75	0.25	0.5	0.5
[27]	0.64	0.36	0.46	0.43
This work	**0.45**	**0.55**	**0.15**	**0.85**

It could still be argued that the photoacoustic signal we attributed to the excitation of PS I centres from the 'mobile' LHCII (b – c in Fig. 2 or 3) is not actually a genuine PS I signal, since we do not provide evidence for its association with a net oxidation of P700. However, we observe the same phenomenon in the wild type and in a mutant lacking the PS II reaction centres. Thus there is no doubt that transition to state 2 involves a large increase of the absorption cross-section of PS I, due to an increased connection with LHCII.

According to the experiment of Fig. 2, the distribution of light excitation among the two photosystems is approximately the following at 650 nm: in state 1, 0.45 for PS II centres and 0.55 for PS I; and in state 2, 0.15 for PS II and 0.85 for PS I. This distribution differs strongly from that reported in Refs. [25–27] for intact leaves, as summarized in Table 3. According to Canaani and Malkin [27], the distribution of light in leaves is considerably far from balance in state 1, whereas in state 2 a near balance of the absorption cross-sections is achieved. Our experiments in *Chlamydomonas* clearly show a quite different situation, where the absorption cross-sections are approximately balanced in state 1 (as in isolated spinach chloroplasts according to [9]), and considerably unbalanced in favour of PS I in state 2. Such a situation seems more consistent with the view that in unicellular green algae, state 1 favours linear electron transfer, whereas state 2 favours cyclic electron transfer around PS I [18,28].

We also note that a 'red drop' beyond 680 nm was reported in other photoacoustic studies [26,27,29]. This is in great contrast with our present observation that the overall quantum yield measured by photoacoustic spectroscopy, in the PS-I-containing strains, reaches its maximum in the far-red region of the spectrum. The modulated light beam used by the authors [26,27,29] probably induced the closure of a large fraction of the PS I centres by generating $P700^+$. In the present work, the weak measuring flash sampled the system in its dark-adapted state, corresponding to the maximal amount of active centres. In other words, the photoacoustic signal was not limited by the turnover of the centres under our experimental conditions.

4.2. Phospho-CP26 is not part of the mobile antenna

The functional data from the present photoacoustic study are consistent with those from optical spectroscopy or fluorescence studies [7,8,28]: they all point to a 50–60% increase of PS I sensitization by LHCII at the expense of PS II upon transition to state 2 in *C. reinhardtii*. This is a much higher value than what has been reported for state transitions from higher plant both in vitro and in vivo [4,6]. There is a striking difference in the phosphorylation patterns of thylakoid membrane proteins between the two types of organism: CP26 and CP29 are reversibly phosphorylated together with LHCII upon state transitions in *C. reinhardtii* but not in higher plants [17]. Whereas the migration of some LHCII, away from PS II, to stroma lamellae regions next to PS I, is well documented both in higher plant and *C. reinhardtii*, the possibility that CP26 and CP29 could also migrate out of the stacked membrane domains had not been examined so far. The present immunocytochemical study, based on lateral distribution of CP26 and LHCII, does not support the idea that minor antenna complexes undergo lateral displacement upon changes in phosphorylation. It is therefore more likely that phosphorylation of minor antenna complexes will contribute, via increased electrostatic repulsion or via an appropriate conformational change (discussed in [4]), to facilitate the detachment of LHCII from PS II, once phosphorylated.

4.3. Immunocytochemical analysis of LHCII lateral distribution leads to an underestimation of LHCII displacement

According to our knowledge on the respective Chl *a* and Chl *b* contents in the various types of chlorophyll-binding protein [30–32], we conclude that about 80% of LHCII is mobile in *C. reinhardtii*, the remaining 20% forming the fixed PS II antenna together with the minor antenna complexes and the core antenna complexes. However, the mobile fraction of LHCII measured by immunocytochemistry (10–20%) is much lower. There are a number of possible interpretations to this apparent discrepancy. Since thylakoids from *C. reinhardtii* do not form well-defined grana [22], accurate selection of stacked and unstacked membrane domains for immunocytochemical analysis might prove more difficult than in higher plants. This drawback may be even more critical if stacked and unstacked regions do not exactly match the respective functional domains for PS II and PS I. There may be energy transfer in state 2 from 'granal' phospho-LHCII to 'stromal' PS I (Ref. [5]). If, in addition, some PS I centres are localized in the margins of the stacked regions, then phospho-LHCII which connects to these centres in state 2 would not be detected as mobile LHCII by immunocytochemical analysis. Such would be the case of PS I α which, according to Svensson et al. [33], accounts for 36% of total PS I in higher plants.

Last but not least, LHCII antigenic sites in the PS II antenna are contributed by each single subunit of LHCII trimers, which are part of clusters of larger oligomers [4]. They will remain densely packed in the stacked membrane domains in the two states, even if the concentration of LHCII varies by a factor of 5. Therefore, one would expect that primary and secondary antibodies will have limited access to these clusters, leading (1) to an underestimation of their content in antigenic sites, and therefrom (2) to a poor sensitivity of the labelling to changes in the internal concentration of antigenic sites in the clusters. This is at variance with the more contrasted situation in unstacked membrane domains, which are almost LHCII-free in state 1 and LHCII-rich in state 2. The net effect of this labelling limitation would be to underestimate the actual changes in LHCII lateral distribution between the two states.

4.4. Supramolecular organization of the light-harvesting antenna in mutants lacking PS II, PS I or cyt b_6f complexes

The present photoacoustic study provided evidence for a change in supramolecular organization of the antenna upon state transitions in mutants lacking the PS II cores, but not in mutants lacking either the PS I cores or the cyt b_6f complexes. However, the last two types of mutant behave very differently. Whatever the conditions, the quantum yield spectrum of cyt b_6f mutants remains typical of state 1. It confirms our previous finding that such mutants do not undergo kinase activation in state 2 conditions [20]. This is in great contrast to PS I mutants, which still show reversible kinase activation. As we discussed previously [34] for the model in which LHCII switches from one photosystem to another upon state transition, no decrease at F_{max} is expected to occur in state 2 when the PS I cores, which act as fluorescence quenchers, are absent. However, as shown by the present immunocytochemical study, some phospho-LHCII may still migrate away from PS II, out of the stacked membrane domains. Functional evidence for this displacement of LHCII arises from the small but significant change in 77 K fluorescence emission ratios. However, the spectra of the quantum yield for charge separation remained strikingly similar and high in the two states (Fig. 7). Since these spectra reflected charge separations occurring in the sole PS II, they could be compared with those of PS II from the wild type. They resembled the state 1 spectrum of PS II, but enhanced by a significant contribution of PS I antenna. This observation is reminiscent of uphill energy transfer from the LHCI peripheral antenna, which was reported to occur in PS I mutants, by Bennoun and Jupin [35] using oxygen evolution measurements. The photoacoustic technique confirms their finding, and the amount of 'uphill' energy transfer computed from the spectra of Fig. 7 is about 25% of the energy absorbed by LHCI, in complete agreement with these authors.Thus a fraction of antenna complexes usually

associated with PS I are connected with PS II, in state 1 as well as in state 2, in PS I mutants. We interpret similarly the status of LHCII in these mutants: it remains connected to PS II in its phosphorylated state, when it would co-localize with LHCI in the wild type (state 2). The basis for this improved association of both LHCI and LHCII with PS II, in the absence of PS I cores, most likely originates from the superstacked organization of the thylakoid membranes in PS-I-deficient mutants (Table 2 and Refs. [22,23]). It would force proteins, which usually partition in unstacked membrane domains – like LHCI or phospho-LHCII – to sit in the stacked membrane domains. Even though some LHCII complexes move towards the periphery of the stacked domains under state 2 conditions, as suggested by the actual increase in LHCII labelling in the small fraction of unstacked membrane domains, the extensive energy transfer which occurs along stacked membrane domains would prevent any significant drop in excitation transfer from phospho-LHCII to PS II centres.

Acknowledgements

We thank D. Béal for his constant help in setting up the photoacoustic device, M. Recouvreur for technical assistance, J. Girard-Bascou and F. Lacquerrière for recovery of double mutants, J.C. Duval (ENS, Paris) and C. Vernotte (CNRS, Gif/Yvette) for the use of their 77 K fluorometers. The BBY particles were obtained by courtesy of F. Rappaport. This work was supported by the CNRS (URA 1187 and UMR 9922), and by contracts BIOCT-930076 to P. Joliot and to F.-A.W.

References

[1] Murata, N. (1969) Biochim. Biophys. Acta 172, 242–251.
[2] Bonaventura, C. and Myers, J. (1969) Biochim. Biophys. Acta 189, 366–383.
[3] Bennett, J. (1991) Annu. Rev. Plant Physiol. 42, 281–311.
[4] Allen, J.F. (1992) Biochim. Biophys. Acta 1098, 275–335.
[5] Georgakopoulos, J.H. and Argyroudi-Akoyunoglou J.H. (1994) Biochim. Biophys. Acta 1188, 380–390.
[6] McCormac, D.J., Bruce, D. and Greenberg, B.M. (1994) Biochim. Biophys. Acta 1187, 301–312.
[7] Wollman, F.-A. and Delepelaire, P. (1984) J. Cell. Biol. 98, 1–7.
[8] Delepelaire, P. and Wollman, F.-A. (1985) Biochim. Biophys. Acta 809, 277–283.
[9] Delosme, R., Béal, D. and Joliot, P. (1994) Biochim. Biophys. Acta 1185, 56–64.
[10] De Vitry, C., Olive, J., Drapier, D., Recouvreur, M. and Wollman, F.-A. (1989) J. Cell. Biol. 109, 991–1006.
[11] Girard, J., Chua, N.-H., Bennoun, P., Schmidt, G. and Delosme, M. (1980) Curr. Gen. 2, 215–221.
[12] Girard-Bascou, J., Choquet, Y., Schneider, M., Delosme, M. and Dron, M. (1987) Curr. Gen. 12, 489–495.
[13] Lemaire, C., Girard-Bascou, J., Wollman, F.-A. and Bennoun, P. (1986) Biochim. Biophys. Acta 851, 229–238.
[14] Bendall, D.S., Sanguansermsri, M., Girard-Bascou, J. and Bennoun, P. (1986) FEBS Lett. 203, 31–35.
[15] Bulté, L. and Wollman, F.-A. (1990) Biochim. Biophys. Acta 1016, 253–258.
[16] Bennoun, P. (1970) Biochim. Biophys. Acta 216, 357–363.
[17] Bassi, R. and Wollman F.–A. (1991) Planta 183, 423–433.
[18] Vallon, O., Bulté, L., Dainese, P., Olive, J., Bassi, R. and Wollman, F.-A. (1991) Proc. Natl. Acad. Sci. USA 88, 8262–8266.
[19] Lemaire, C., Girard-Bascou, J. and Wollman, F.-A. (1986) in Progress in Photosynthesis Research (Biggins, J., ed.), Vol. 4, pp. 655–658, Martinus Nijhoff, Dordrecht.
[20] Wollman, F.-A. and Lemaire, C. (1988) Biochim. Biophys. Acta 933, 85–94.
[21] Wollman, F.-A. and Bennoun, P. (1982) Biochim. Biophys. Acta 680, 352–360.
[22] Goodenough, U.W. and Levine, R.P. (1969) Plant Physiol. 44, 990–1000.
[23] Baldan, B., Girard-Bascou, J., Wollman, F.-A. and Olive, J. (1991) J. Cell. Biol. 114, 905–915.
[24] Allen, J.F. and Melis, A. (1988) Biochim. Biophys. Acta 933, 95–106.
[25] Veeranjaneyulu, K., Charland, M., Charlebois, D. and Leblanc, R.M. (1991) Plant Physiol. 97, 330–334.
[26] Veeranjaneyulu, K. and Leblanc, R.M. (1994) Plant Physiol. 104, 1209–1214.
[27] Canaani, O. and Malkin, S. (1984) Biochim. Biophys. Acta 766, 513–524.
[28] Bulté, L., Gans, P., Rébeillé, F. and Wollman, F.-A. (1990) Biochim. Biophys. Acta 1020, 72–80.
[29] Malkin, S., Herbert, S.K. and Fork, D.C. (1990) Biochim. Biophys. Acta 1016, 177–189.
[30] Jennings, R.C., Bassi, R., Garlaschi, F.M., Dainese, P. and Zucchelli, G. (1993) Biochemistry 32, 3203–3210.
[31] Zucchelli, G., Dainese, P., Jennings, R.C., Breton, J., Garlaschi, F.M. and Bassi, R. (1994) Biochemistry 33, 8982–8990.
[32] Bassi, R., Soen, S.Y., Frank, G., Zuber, H. and Rochaix, J.D. (1992) J. Biol. Chem. 267, 25714–25721.
[33] Svensson, P., Andreasson, E. and Albertsson, P.Å. (1991) Biochim. Biophys. Acta 1060, 45–50.
[34] Bulté, L. and Wollman, F.-A. (1989) in Photoconversion Processes for Energy and Chemicals (Hall, D.O. and Grassi, G., eds.), pp. 198–207, Elsevier, Amsterdam.
[35] Bennoun, P. and Jupin, H. (1976) Biochim. Biophys. Acta 440, 122–130.